D. Feng, F. Aymerich, Effect of core density on the low-velocity impact response of foam-based sandwich composites, Composite Structures, Volume 239, 1 May 2020, 112040

EFFECT OF CORE DENSITY ON THE LOW-VELOCITY IMPACT RESPONSE OF FOAM-BASED SANDWICH COMPOSITES

D. Feng[1], F. Aymerich[2]*

[1] College of Civil Engineering, Taiyuan University of Technology, Shanxi 030024, China
e-mail: fengdianshi@tyut.edu.cn

[2] Department of Mechanical, Chemical and Materials Engineering, University of Cagliari, 09123 Cagliari, Italy
e-mail: francesco.aymerich@dimcm.unica.it

ABSTRACT

The paper presents the results of an investigation into the effect of core density on the low-velocity impact response of foam-based sandwich composites. Drop-weight tests were conducted on sandwich panels with carbon/epoxy facesheets and a 10 mm thick PVC foam core. Three foam core densities (65, 100 and 160 kg/m^3) and two facesheet layups ($[0/90_3/0]$, $[0_3/\pm45]_S$) were examined in the study. The analyses show that the influence of core density on the damage resistance of the panels is strongly correlated to the layup of the skin. While the damage developing in $[0/90_3/0]$ panels is not affected by core density, the damage area in $[0_3/\pm45]_S$ panels reduces with increasing core density. The different influence of core properties on the damage response of $[0/90_3/0]$ and $[0_3/\pm45]_S$ sandwich panels may be attributed to the different bending stiffness of the facesheets, with a response to impact dominated by global bending in panels with thin $[0/90_3/0]$ skins as opposed to one mainly governed by local shear rigidity in panels with thicker $[0_3/\pm45]_S$ skins. FE analyses were finally carried out to assess the capability of a model developed by the authors to capture the role of foam density in the impact damage response of the panels.

Keywords: Sandwich composites; Core density; Impact behaviour; Damage; Finite element analysis

1. INTRODUCTION

Composite sandwich structures have been increasingly used in aerospace, marine, wind energy and civil engineering fields, because of a number of significant advantages over more conventional materials, such as high specific strength and stiffness, excellent energy-absorbing properties, good fatigue and corrosion resistance [1-4]. A typical sandwich structure consists of two stiff and strong facesheets (skins) separated by a thick low-density core. The facesheets are designed to carry bending and in-plane loads, while the core is responsible for sustaining transverse shear loads and stabilizing and supporting the facesheeets. Polymeric foam cores, in particular, have gained considerable interest in recent years [5-6], owing to their low cost, easy manufacturing processes, good moisture resistance and superior thermal and sound insulation properties. In addition, a number of polymeric foams, such as those based on polyvinyl chloride (PVC), polyurethane (PU) or polymethacrylimide (PMMI), are suitable for autoclave consolidation and co-curing techniques, where the prepreg facesheets are cured and bonded to the core in a single step.

A major limitation of sandwich composites is their high vulnerability to low-velocity impacts, which may occur during the various stages of the life of a structure, including manufacturing, transportation, installation and maintenance. The damage induced by low-velocity impact usually consists of a complex combination of multiple failure modes involving delamination, matrix cracking, fibre breakage, core crushing and face-core debonding [7]. Although the damage may be difficult to detect by visual inspection, it can significantly reduce (up to more than 70%) the residual load-carrying capacity of the structure [7-9]. A good knowledge of the response to impact of composite sandwich structures is thus strongly needed for the development and validation of reliable design and selection procedures for this class of materials.

* Corresponding author

A large and growing body of literature is available on the characterization and prediction of the behaviour of monolithic laminated composites under low-velocity impact. In contrast, much less work has been carried out on the investigation of the response to impact, and of the related damage processes, of sandwich composites with polymer foam cores, in which additional complexity is introduced by the interaction between the degradation mechanisms of face sheets and foam core [10-15]. In particular, a very limited number of studies have specifically addressed the effect of foam core density on the structural properties and damage mechanisms of sandwich structures subjected to low-velocity impact loads [13, 16-21].

The impact response of sandwich composites made of glass fibre facesheets and PVC foam cores with different densities was examined by Caprino and Teti [16], who found that the damage induced by impact was substantially independent of the density of the core, in spite of the fact that, as expected, the maximum contact force increased with increasing core density.

Conversely, Anderson and Madenci [17] reported higher damage resistance, with damage more localized in the vicinity of the impact site, in carbon facesheet/PMMI foam sandwich panels with a high-density core as compared to analogous low-density foam panels. Similarly, the failure of the impacted facesheet was seen to be dependent on the properties of the core material by Cantwell and coworkers [18, 19], who investigated the impact resistance of sandwich panels manufactured with PVC, PU or PET (polyethylene terephthalate) foam cores with different densities. Both the threshold energy for damage initiation [18] and the perforation energy [19] were in particular observed to increase with increasing foam density; as an example, sandwich panels with 200 kg/m^3 PVC cores showed a perforation resistance eight times higher than that of panels with a core density of 60 kg/m^3.

Atas and Sevim [20] compared the impact behaviour of sandwich composites combining glass fibre skins with PVC foam or balsa cores, with densities of 62 kg/m^3 and 157 kg/m^3, respectively. The experimental tests showed that impacts on PVC foam sandwich specimens resulted in larger deflections and more extensive delamination areas than those on corresponding balsa foam sandwich samples, as a likely consequence of the much lower stiffness of the PVC core material. Similar findings may be found in [9, 21, 22], which report that the resistance to impact or indentation damage of foam-based sandwich composites was generally improved by increasing the stiffness and strength of the core.

It should be noted, however, that a reduction in damage resistance, with an increase in impact delamination area, was on the contrary observed by Long et al. [23] in carbon sandwich panels when increasing the density of the PU foam core from 52 kg/m^3 to 75 kg/m^3.

The published research work thus reports somewhat conflicting and apparently contradicting experimental results on the influence of core density on the impact damage response of foam-based sandwich panels; further analyses are therefore needed to explore and clarify the correlation between core properties and damage modes induced by impact in composite sandwich structures.

The aim of this paper is to investigate the low-velocity impact behaviour of sandwich panels with different core densities, in order to characterize, and possibly predict, the effect of foam core properties on the mechanical response and on the damage resistance of the sandwich structures. The attention has been focused on the examination of the response to impacts that induce barely visible impact damage (BVID) in the composite skins, which is of particular concern for the safety and in-service structural integrity of composite sandwich composites [9, 12, 24].

In this study, a series of drop-weight tests and damage evaluation analyses were carried out at increasing impact energies on sandwich panels that combine carbon/epoxy facesheets in two different layups with PVC foam cores of three densities. A numerical tool previously developed by the authors was used to predict the structural response and the damage evolution observed during the experimental analyses. The simulation results are compared with the experimental findings in terms of force vs deflection curves as well as of size, shape, and distribution of internal damage to assess the quality of the numerical simulations for impacts on sandwich panels with different foam properties and facesheet layups.

2. EXPERIMENTAL

Sandwich panels with in-plane dimensions of 250 mm × 250 mm and a 10 mm thick PVC foam core were manufactured with two different facesheet layups ($[0/90_3/0]$ and $[0_3/\pm45]_S$, with thicknesses of 1.6 mm and 3.2 mm, respectively) and three different foam densities, ranging from 65 kg/m^3 to 160 kg/m^3. The skins of the sandwich panels were made with prepreg layers of unidirectional Seal Texipreg® HS300/ET223 carbon/epoxy, which is a prepreg tape suitable for vacuum-bag-only processing at curing temperatures ranging between 85°C and 125°C. Individual plies had a fibre volume ratio of 0.62 and a nominal thickness of 0.32 mm. The core was made of DIAB Divinycell® HP PVC foams, which are high temperature, closed-cell foam grades with high compatibility with low-medium temperature prepreg systems [25]. PVC foams with densities of 65 kg/m^3 (HP60), 100 kg/m^3 (HP100) and 160 kg/m^3 (HP160) were used in the investigation.

The sandwich panels were consolidated in a vacuum-bag by a co-curing process, in which the prepreg layers were simultaneously cured and bonded to the core without using any additional adhesive material. The curing cycle consisted of a 3°C/min heating stage, followed by a 6 h dwell at 100°C and a cooling stage back to room temperature while maintaining vacuum.

The strength and fracture properties of the prepreg material were characterized in previous studies [26], while flatwise transverse compression tests were performed on foam samples at a nominal strain rate of 0.1/s to assess the compressive properties of the different foam grades. The stress-strain curves obtained for the different foam densities (Fig. 1) exhibit an initial linear elastic region, followed by a long stress plateau, associated with the buckling of the cell walls (crushing), and by a final steep increase in stiffness, corresponding to the compaction of the material (densification stage) [27]. The plots of Fig. 1 clearly show that the mechanical response of the foam is highly dependent on its density, with increases in foam density resulting in significant increases in elastic modulus and plateau stress.

Impact tests were carried out using an instrumented drop-weight testing machine equipped with a 2.34 kg hemispherical impactor, provided with an indentor 12.5 mm in diameter. The sandwich panels were simply supported on a steel plate with a 45.0 mm × 67.5 mm rectangular opening and subjected to impacts ranging between 1 J and 9 J, obtained by varying the drop height of the impactor. At least three specimens were tested at each impact energy level for all examined sandwich configurations. The contact force during the impact was measured by a strain-gauge bridge bonded to the indentor, while the velocity of the impactor immediately before the contact was obtained by an infra-red sensor. The deflection experienced by the impacted skin during the impact was estimated by numerical integration of the force-time trace. Impact-induced damage was finally assessed by penetrant-enhanced X-radiography of the impacted facesheet and qualitatively evaluated by optical microscopy on polished cross-sections.

3. EXPERIMENTAL RESULTS AND DISCUSSION

3.1 Effect of core density on the structural response

Fig. 2 and Fig. 3 show typical impact force histories and force-deflection curves acquired for impacts of 6.2 J on the different sandwich panel configurations. As expected, because of the larger thickness and flexural rigidity of the facesheets, sandwich panels with $[0_3/\pm45]_S$ skins exhibit a significantly stiffer response than analogous $[0/90_3/0]$ panels. The plots also show that the density of the core material significantly affects the structural behaviour of the sandwich panel for both $[0/90_3/0]$ and $[0_3/\pm45]$s skin layups. It is seen that an increase in foam density results in a marked increase in force vs deflection slope and in maximum impact force, as well as in a decrease in impact duration and maximum deflection. As an example, the peak contact force increases of about 10% and 25% when the core density is increased from the lower 65 kg/m^3 value to 100 kg/m^3 and 160 kg/m^3, respectively.

As shown in Fig. 3, the force-displacement plots have an approximately linear (elastic) behaviour up to a load of about 1 kN for $[0/90_3/0]$ panels and 2 kN for $[0_3/\pm45]_S$ panels; above this knee point the curves show a stiffness decrease that is caused, as will be detailed in the following section, by damage and degradation phenomena occurring in the laminated skin and in the core. It should be observed that the response measured just after the first contact is affected by oscillations and fluctuations, which are signal features typical of impact force data and due to the inertial and dynamic behaviour of the panel-impactor system [19, 28]. These effects are particularly pronounced in the impact force signals of sandwich panels with stiffer $[0_3/\pm45]_S$ skins, which exhibit initial oscillations characterized by larger amplitudes for higher core densities (see Figs. 2b and 3b).

To further compare the influence of core density on the structural impact performance of the examined sandwich structures, the values of the peak force and of the energy absorbed during impact, which are global indicators usually adopted to characterize the impact behaviour of composite materials [2], are plotted as a function of impact energy in the graphs of Figs. 4 and 5. The absorbed energy value, calculated as the area enclosed within the force-deflection curve, may be assumed as an indicator of the energy dissipation performance of the structure. The data reported in the graphs show that while the maximum impact forces increase with increasing foam density (Fig. 4), the energy absorption capacities of the sandwich structures are practically independent of the density of the core for both $[0/90_3/0]$ and $[0_3/\pm45]_S$ sandwich panels (Fig. 5). We may also observe that the absorbed energy values are significantly lower than the corresponding impact energy values (the equality between impact energy and absorbed energy is represented by the dotted straight line in the graphs of Fig. 5); this result was expected, as the range of investigated impact energies is associated to barely visible impact damage (BVID) scenarios and is therefore rather distant from the perforation energy threshold, which would correspond to equal absorbed and impact energies [29].

3.2 Effect of core density on the internal damage

Fig. 6 shows X-radiographs of internal impact damage in the composite facesheets of $[0/90_3/0]$ (Fig. 6a) and $[0_3/\pm45]_S$ (Fig. 6b) sandwich panels with the HP60, HP100 and HP160 cores. X-ray and microscopy analyses indicate that, for all examined configurations, the damage induced by impact consists of a combination of tensile/shear matrix cracks, delaminations and fibre failure [15]. However, because of the difference in layup, $[0/90_3/0]$ and $[0_3/\pm45]_S$ facesheets exhibit rather different damage patterns when subjected to similar impact energies.

In $[0/90_3/0]$ panels (Fig. 6a), the damage initiates in the form of bending matrix cracks in the 0º layer farthest from the impact side and shear matrix cracks in the middle 90º layers; with increasing impact energy, these matrix cracks promote the development of a two-lobe delamination at the lowermost 90º/0º interface between the cracked 0°and 90° plies. Small delaminations were observed on the top 0°/90° interface only for impact energies larger than 4 J. No major fibre damage was detected in the impacted skin in the full range of investigated impact energies (1 J - 8 J). It is worth remarking that the onset and evolution of the main damage mechanisms observed in the impacted skins are not altered by the density of the foam material used in the core.

In $[0_3/\pm45]_S$ panels (Fig. 6b), damage initiates with a large bending matrix crack in the bottom 0º layers, immediately followed by a delamination on the -45º/+45º interface and fine matrix cracking in the +45º plies. With increasing impact energies, delaminations tend to initiate and grow at all remaining interfaces between plies with different orientations, in association with matrix cracking in adjacent layers. Minor fibre damage, developing at the indentation area in the top 0º layer, is only observed for impact events with energies higher than about 6 J. The nature of the typical damage modes is again not evidently affected by the density of the core.

A comparative analysis of X-radiographs and force-time curves for different impact energies shows that, for both $[0/90_3/0]$ and $[0_3/\pm45]_S$ sandwich panels, only minor damage occurs in the composite facesheets at the load level corresponding to the knee point of the force-displacement curves. At the same time, microscopy inspections showed no evidence, for all core densities, of major damage phenomena within the foam (such as large cavities or fractured cell walls) or of debonding between the core and the skin, even when the sandwich panels were impacted at the highest impact energies. These observations suggest that the stiffness reduction exhibited by the sandwich panels at the knee load is mainly induced by nonlinearities associated to localized cell buckling of the foam material below the indentation area, rather than by major damage in the composite skins.

If we focus on the influence of core density, examination of the damage occurring in the sandwich panels as revealed by X-radiography shows that the extent of damage occurring in thin $[0/90_3/0]$ skins is not significantly affected by the properties of the core material (Fig. 6a). In sandwich composites with thicker $[0_3/\pm45]_S$ skins, in contrast, the size of the damage area generated by the impact decreases as the core density increases. It should be noted that this reduction in overall damage size occurs in spite of the higher impact force experienced by high-density core sandwich panels as compared to low-density core panels. The influence of foam core density on damage initiation and damage size of $[0/90_3/0]$ and $[0_3/\pm45]_S$ sandwich panels is illustrated in the graphs of Fig. 7, which compare the projected damage areas (defined as the projection onto a single plane of the delaminated areas at all interfaces of the impacted skin) as a function of impact energy, for all foam density panels. The data concerning the response of $[0_3/\pm45]_S$ sandwich panels (Fig. 7b) show, in particular, that while the resistance to damage initiation is independent of core density (the energy threshold for damage onset is about 1 J for all densities, see Fig. 6b), the overall damage size reduces with increasing core density for impact energies higher than this threshold level, with the extent of this reduction rising with increasing impact energy.

The different effect of foam core density on the damage resistance of the two classes of sandwich panels may be attributed to the significantly different stiffness of the laminated facesheets. The impact and damage response of sandwich panels with the thicker $[0_3/\pm45]_S$ skins is controlled by the local shear rigidity rather than by the global flexural stiffness of the impacted facesheet, as already observed in [16]. The increased support provided by a denser and stiffer core to the localized indentation occurring during the impact results thus in a reduction of the overall damage area in comparison to lower density cores.

In sandwich composites with thinner $[0/90_3/0]$ facesheets, in contrast, the impacted skin experiences significant global bending and, under increasing deflections, the stress state of the facesheet is increasingly dominated by membrane stresses [30], as also confirmed by the increasing slope of force-deflection curves of this class of sandwich panels (see Fig. 3a). In sandwich structures with thin facesheets, because of the presence of significant membrane load contributions, the role played by the supporting core is therefore not as crucial as in the case of thick facesheets, and this explains why the introduction of denser and more rigid cores does not essentially affect the damage response of $[0/90_3/0]$ sandwich composites.

4. NUMERICAL SIMULATIONS

The experimental observations illustrated in the previous section were finally compared to the results of an FE tool recently developed by the authors for the simulation of impact events in sandwich and laminated composites [14, 26]. The comparisons were used to assess the accuracy of the simulations for the different sandwich configurations examined in the study and to verify the ability of the model to correctly capture and reproduce the effect of different foam densities on the damage response of the impacted structures.

The model simulates the initiation, growth and interaction of the failure modes developing in the composite skins (matrix cracks, fibre fracture and delamination) by energy-based continuum damage mechanics models for intralaminar damage and by implementing a cohesive behaviour at the ply interfaces for interlaminar damage [26]. The intralaminar damage models used in the FE analyses are based on the assumptions that the damage process is smeared over the finite element dimension and that the material degradation is quantified by introducing a set of internal damage variables specific to each type of fibre or matrix failure. The degradation is applied on a ply-by-ply basis and leads to the reduction of the relevant material stiffnesses. The interface cohesive elements, used for simulating the delaminations between layers of the composite skins and possible debonding between skins and core, employ a bilinear constitutive law for describing the relation between tractions and separations at the interfaces. The behaviour of the interface is linear elastic until a stress-based damage initiation criterion is satisfied, followed by a linear softening phase that defines the progressive decohesion of the interface with increasing separation. The damage models described above were implemented into ABAQUS/Explicit through user-defined material subroutines VUMAT.

The nonlinear behaviour of the foam core was modelled using the crushable foam plasticity model with volumetric hardening available in ABAQUS, where the hardening behaviour is represented in terms of uniaxial compressive stress versus plastic strain. The compressive stress-strain curves measured for the three different PVC foam densities, as previously plotted in Fig. 1, were used to define the piecewise linear hardening laws provided as input data to the crushing model.

A typical FE model of the sandwich panels, which was solved in ABAQUS using an explicit integration procedure, is shown in Fig. 8. The sandwich panels have been modeled using C3D8R solid elements for the composite skins and the foam core, and using zero-thickness COH3D8 cohesive elements at the interfaces between skin layers with different fibre orientations and between skins and core to simulate delamination and core/skin debonding, respectively. An explicit solver was used to analyze the impact events, and nonlinear effects due to large deformation were included in the solution process by activating the NLGEOM option.

Further details of the FE tool and on the experimental tests carried out to obtain the material properties used in the analyses may be found in [14, 26].

Fig. 9 compares the force-time and force-displacement curves predicted by the FE model with those acquired experimentally during 1 J and 6.2 J impacts on $[0/90_3/0]$ sandwich panel. The model is able to reproduce with very good accuracy the structural response of the panels, and to correctly capture the effect of core density on the main characteristics of the impact curves, such as the increase in stiffness and peak load and the decrease in impact time with increasing core density. The load level of the knee point above which a clear slope reduction is observed (about 1 kN), is also correctly predicted by the FE simulations. Quantitative comparisons of predicted and measured peak contact forces and absorbed energies are shown in Fig. 10 for panels with HP60, HP100 and HP160 foam cores. The graphs show that there is a very good correlation between numerical predictions and experimental data, with only a slight tendency of the FE model to underpredict the maximum force values for high-energy impacts on HP160 sandwich panels.

Experimental and numerical results for sandwich panels of different foam densities are compared in Fig. 11 in terms of damage occurring in the composite skins at different impact energies. Fig. 11a reports experimental and predicted values of projected damage area, while the graphs of Fig. 11b plot the length (maximum size along 0º direction) and width (maximum size along 90º direction) of the projected damage. Typical images of projected damage areas as revealed by X-radiography and predicted by FE simulation are shown side by side in Fig. 12. The comparisons show that the FE analyses predict with acceptable accuracy the total damage area and the trends of the damage length and damage width with increasing impact energy, even though the width of the delaminated area tends to be generally overpredicted by the model.

The numerical analyses also provide a correct description of the sequence of the major damage events and of the features and shapes of the individual damage modes occurring through the thickness of the sandwich panels. As an example, Fig. 13 shows different stages of damage evolution as simulated by the FE model during a 7.8 J impact on a HP160-base sandwich plate. The numerical simulation indicates that a localized area of foam core beneath the impact point reaches the plateau stress stage (where plastic strain of the foam increases at a nearly constant compressive stress) at an impact force level of about 1 kN, while only a small amount of matrix cracking is predicted in 90° layers of the laminated facesheet; the numerical results are in agreement with experimental evidence, which indicates, as remarked in the previous section, that the stiffness reduction exhibited by the force-displacement curves at the knee load is mainly induced by localized cell buckling of the foam material, rather than by damage of the composite skin. The development of a major bending matrix crack in the bottom 0° layer, a two-lobe delamination at the lower 90°/0° interface and a smaller delamination at the upper 0°/90° interface are subsequently predicted by the model with increasing contact force. In accordance to experimental observations, no fibre breakage in the laminated skin and no debonding at the core/skin interface is predicted by the model.

The structural responses of $[0_3/\pm45]_S$ sandwich composite panels obtained by FE simulations are compared with experimental data in Fig. 14. A good correlation is again obtained between FE simulations and experiments in terms of force-time and force-displacement relationships for all three core densities. In accordance to experiments, the developed FE model is capable of reproducing the characteristic nonlinearities and the sudden stiffness drop occurring at a threshold load of about 2 kN. The good match between experiments and predictions can also be confirmed by the comparisons illustrated in the graphs of Fig. 15, which plot the maximum contact force and the energy absorbed during impact for sandwich composites with the three core densities, even though some discrepancies in energy absorption may be noticed at high impact energies for HP 100 and HP160 panels.

Comparisons between experiments and predictions in terms of damage occurring in composite skins at various impact energies for HP60, HP100 and HP160 sandwich panels are illustrated in Fig. 16, while Fig. 17 reports images of projected damage areas as revealed by X-radiography and reconstructed by FE simulation. As shown by these results, the FE model accurately predicts the size (Fig. 16a) and shape (Fig. 17) of overall damage induced by impact for the different foam densities, correctly capturing the decrease in damage size with increasing core density. The model is also able to reproduce, for the different core densities, the different rates of growth with impact energy of the total damage along the 0° (damage length) and 90° (damage width) directions, with higher densities corresponding to lower growth rates (Fig. 16b).

Fig. 18 shows an example of individual damage modes predicted at various stages during an 8.5 J impact on an HP60-based panel. In agreement with experimental observations, a very little amount of damage in the composite skins (i.e. only a small bending matrix crack in the bottom 0° layers) is predicted by the FE model at a load of about 2 kN, while a considerable region of the foam core (spread in an elliptical shape elongated along the 0º direction) has reached the plateau stage at the characteristic knee load. The results again confirm the assumption that foam crushing plays a major role in the rapid stiffness drop recorded during the impact event upon reaching the knee load level. Delaminations initiate at the middle +45°/-45° and -45°/+45° interfaces and, under increasing load, they also develop and grow at the remaining interfaces, together with associated matrix damage in 0° and ±45° layers. Localized fibre fracture is finally predicted in the indentation area of the top 0°

layers for a load of about 4.5 kN, and a slight decrease of stiffness can be observed correspondingly on the force-displacement curve. In accordance with experimental findings, no delamination is predicted by the model at the interface between the core and the face skin over the entire range of impact energies investigated.

5. CONCLUSION

The effect of core density on the structural and damage performance of foam-based sandwich composites subjected to low-velocity impact was examined in the paper. Drop-weight tests were carried out on different configurations of sandwich panels consisting of PVC foam cores with three densities (65 Kg/m^3, 100 Kg/m^3 and 160 Kg/m^3) and carbon/epoxy laminated facesheets with $[0/90_3/0]$ and $[0_3/\pm45]_S$ layups. The predictions of a FE tool previously developed by the authors were finally compared to the experimental results to assess the ability of the model to correctly predict the mechanical behaviour and to faithfully reproduce the nature and progression of damage mechanisms in the facesheets of sandwich panels with different cores.

The main findings of the study can be summarized as follows:

- The density of the foam core significantly affects the structural response to impact, as described by force-time and force-deflection curves, of both $[0/90_3/0]$ and $[0_3/\pm45]_S$ panels, with increases in core density resulting in larger force-deflection slopes, higher peak loads and shorter impact durations. Conversely, the energy dissipated during impact appears to be substantially independent of the core density.
- Core crushing at the impacted region is the primary cause of the stiffness drop recorded during impact upon reaching the knee point of the force-displacement curve.
- The effect of core density on the damage induced by impact in the composite skins is dependent on the skin layup.
    - Impact damage in the skins of $[0/90_3/0]$ sandwich structures, including the nature of individual damage modes, their initiation and propagation, as well as the size of overall damage, is not influenced by the density of the foam core over the entire range of examined impact energies.
    - In $[0_3/\pm45]_S$ panels, in contrast, while the threshold energy for damage initiation is not affected by core density, the damage area reduces with increasing core density for higher impact energies.

  The different influence of core density on the damage resistance of $[0/90_3/0]$ and $[0_3/\pm45]_S$ sandwich panels may be attributed to the largely different flexural stiffness of the facesheets, which results in a response to impact controlled by global bending in panels with thin $[0/90_3/0]$ skins as opposed to a deformation behaviour dominated by local shear rigidity in panels with thicker $[0_3/\pm45]_S$ skins.
- The results of the FE analyses are in good agreement with the experimental findings and demonstrate the capability of the proposed FE model to accurately predict the structural behaviour and the damage response of impacted sandwich panels, and to properly capture the influence of core properties and facesheet layups on impact damage in terms of initiation, evolution, shape and extent of the different failure mechanisms.

ACKNOWLEDGEMENTS

The research described in this paper was financially supported by the EU funded FP7-ITN-Marie Curie project SYSWIND (Grant No. FP7-PEOPLE-ITN 238325). The first author would also like to thank the support by Scientific and Technological Innovation Programs of Higher Education Institutions in Shanxi (2019L0203).

Data Availability

The raw data required to reproduce these findings are available to download from the Mendeley Data repository

REFERENCES

[1] Thomsen OT, Sandwich Materials for Wind Turbine Blades - Present and Future. Journal of Sandwich Structures and Materials 2009; 11: 7-26.

[2] Mohamed M, Anandan S, Huo Z, Birman V, Volz J, Chandrashekhara K, Manufacturing and characterization of polyurethane based sandwich composite structures, Composite Structures 2015; 123: 169-179.

[3] Birman V, Kardomateas GA, Review of current trends in research and applications of sandwich structures, Composites Part B: Engineering 2018; 142: 221-240.

[4] Elamin M, Li B, Tan, KT, Impact damage of composite sandwich structures in arctic condition, Composite Structures 2018; 192: 422-433..

[5] Siriruk A, Weitsman JY, Penumadu D, Polymeric foams and sandwich composites: Material properties, environmental effects, and shear-lag modeling. Composites Science and Technology 2009; 69(6): 814–820.

[6] Fathi A, Wolff-Fabris F, Altstädt V, Gätzi R, An investigation on the flexural properties of balsa and polymer foam core sandwich structures: Influence of core type and contour finishing options. Journal of Sandwich Structures & Materials 2013; 15(5): 487-508.

[7] Abrate S, Localized impact on sandwich structures with laminated facings. Applied Mechanics Reviews 1997; 50: 69-97.

[8] Schubel PM, Luo JJ, Daniel IM, Impact and post impact behavior of composite sandwich panels. Composites Part A: Applied Science and Manufacturing 2007; 38(3): 1051-1057.

[9] Leijten J, Harald EN Bersee, Bergsma OK, Beukers A. Experimental study of the low-velocity impact behaviour of primary sandwich structures in aircraft. Composites Part A: Applied Science and Manufacturing 2009; 40(2): 164-175.

[10] Belingardi G, Cavatorta MP, Duella R, Material characterization of a composite–foam sandwich for the front structure of a high speed train. Composite Structures 2003; 61: 13-25.

[11] Xia F, Wu X, Work on low-velocity impact properties of foam sandwich composites with various facesheets. Journal of Reinforced Plastics and Composites 2010; 29(7):1045-1053.

[12] Chai GB, Zhu ,. A review of low-velocity impact on sandwich structures. Proceedings of the Institution of Mechanical Engineers, Part L: Journal of Materials: Design and Applications 2011; 225(4): 207–230.

[13] Daniel, IM, Abot JL, Schubel PM, Luo JJ, Response and damage tolerance of composite sandwich structures under low velocity impact. Experimental Mechanics 2012; 52(1): 37-47.

[14] Feng D, Aymerich F, Damage prediction in composite sandwich panels subjected to low velocity impact, Composites Part A: Applied Science and Manufacturing 2013; 52: 12-22.

[15] Feng D, Aymerich F, Experimental and numerical investigation into the damage response of composite sandwich panels to low-velocity impact. Structural Monitoring and Maintenance 2017; 4(2):133-151.

[16] Caprino G, Teti R, Impact and post-impact behavior of foam core sandwich structures. Composite Structures 1994; 29(1):47-55.

[17] Anderson T, Madenci E, Experimental investigation of low-velocity impact characteristics of sandwich composites. Composite Structures 2000; 50(3): 239-247.

[18] Hazizan MA, Cantwell WJ, The low velocity impact response of foam-based sandwich structures. Composites Part B: Engineering 2002; 33(3): 193-204.

[19] Zhou J, Hassan MZ, Guan Z, Cantwell WJ, The low velocity impact response of foam-based sandwich panels. Composites Science and Technology 2012; 72(14):1781–1790.

[20] Atas C, Sevim C, On the impact response of sandwich composites with cores of balsa wood and PVC foam. Composite Structures 2010; 93(1): 40-48.

[21] Daniel IM, Impact Response and Damage Tolerance of Composite Sandwich Structures, in Shukla A, Ravichandran G, Rajapakse Y (Eds.), Dynamic failure of materials and structures. Springer; 2010.

[22] Flores-Johnson EA, Li QM. Experimental study of the indentation of sandwich panels with carbon fibre-reinforced polymer face sheets and polymeric foam core. Composites Part B: Engineering 2011; 42(5): 1212-1219.

[23] Long S, Yao X, Wang H, Zhang X, Failure analysis and modeling of foam sandwich laminates under impact loading. Composite Structures 2018; 197: 10-20.

[24] Vaidya UK, Impact response of laminated and sandwich composites, in Impact Engineering of Composite Structures, Abrate S (Ed.). Springer; 2011.

[25] Divinycell,Technical Data Sheet, HP-grade, DIAB, Laholm, Sweden, 2005

[26] Feng D, Aymerich F. Finite element modelling of damage induced by low-velocity impact on composite laminates. Composite Structures 2014; 108: 161-171

[27] Gibson LJ, Ashby MF. Cellular solids: structure and properties. Cambridge University Press; 1999.

[28] Feraboli P, Some recommendations for characterization of composite panels by means of drop tower impact testing. Journal of Aircraft 2006; 4(6): 1710-1718.

[29] Belingardi G, Cavatorta MP, Paolino DS, Repeated impact response of hand lay-up and vacuum infusion thick glass reinforced laminates. International Journal of Impact Engineering 2008; 35(7): 609-619.

[30] Olsson R, Analytical prediction of large mass impact damage in composite laminates. Composites Part A: Applied Science and Manufacturing 2001; 32(9): 1207-1215.

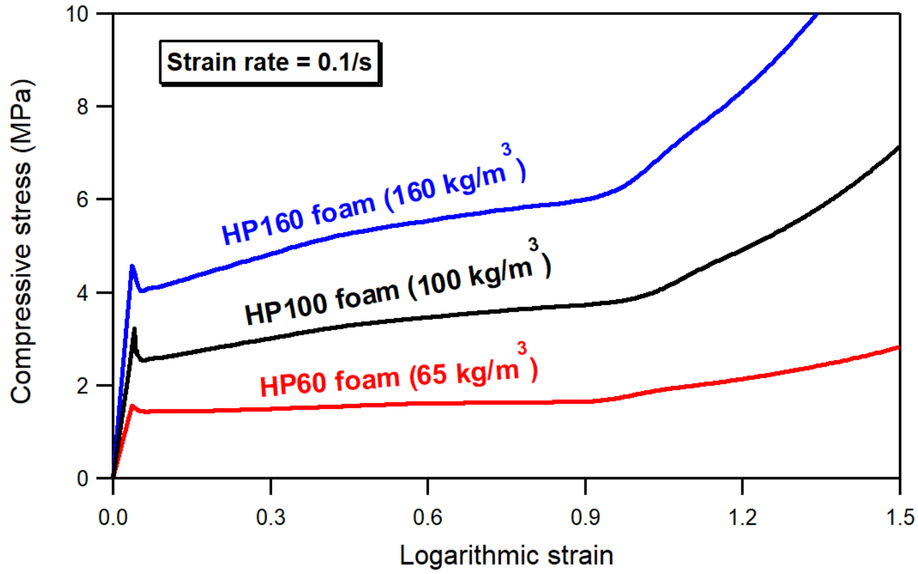

Figure 1: Stress-strain curves of PVC foam under uniaxial compression.

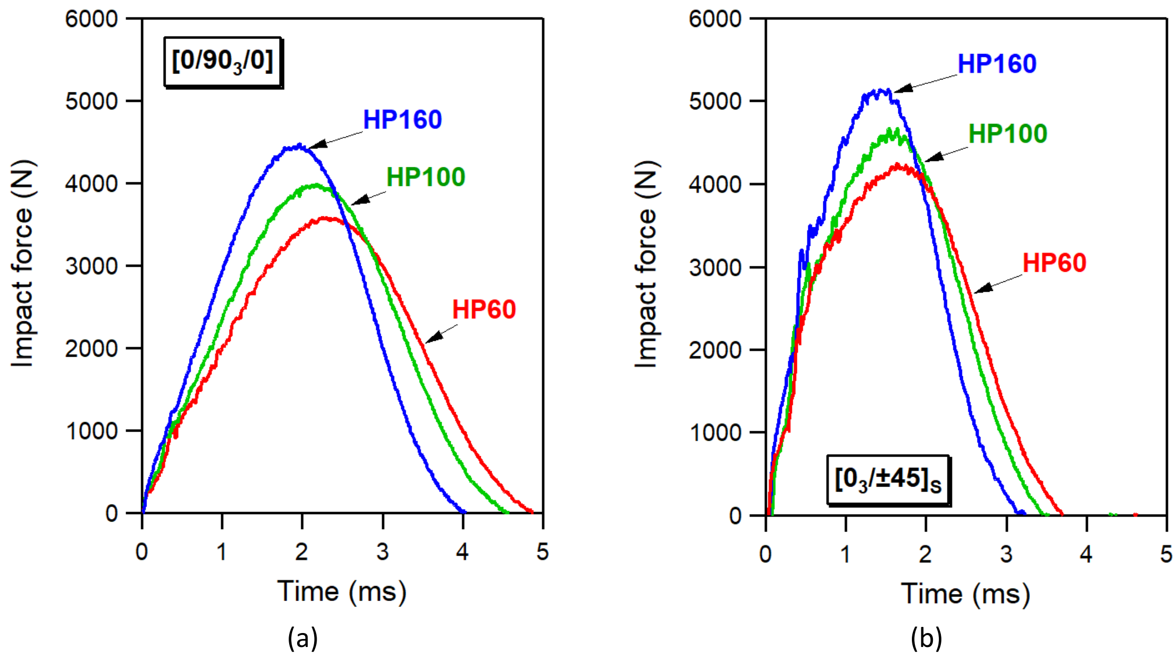

Figure 2: Force-time curves of $[0/90_3/0]$ (a) and $[0_3/\pm45]_S$ (b) sandwich panels with different core densities for a 6.2 J impact

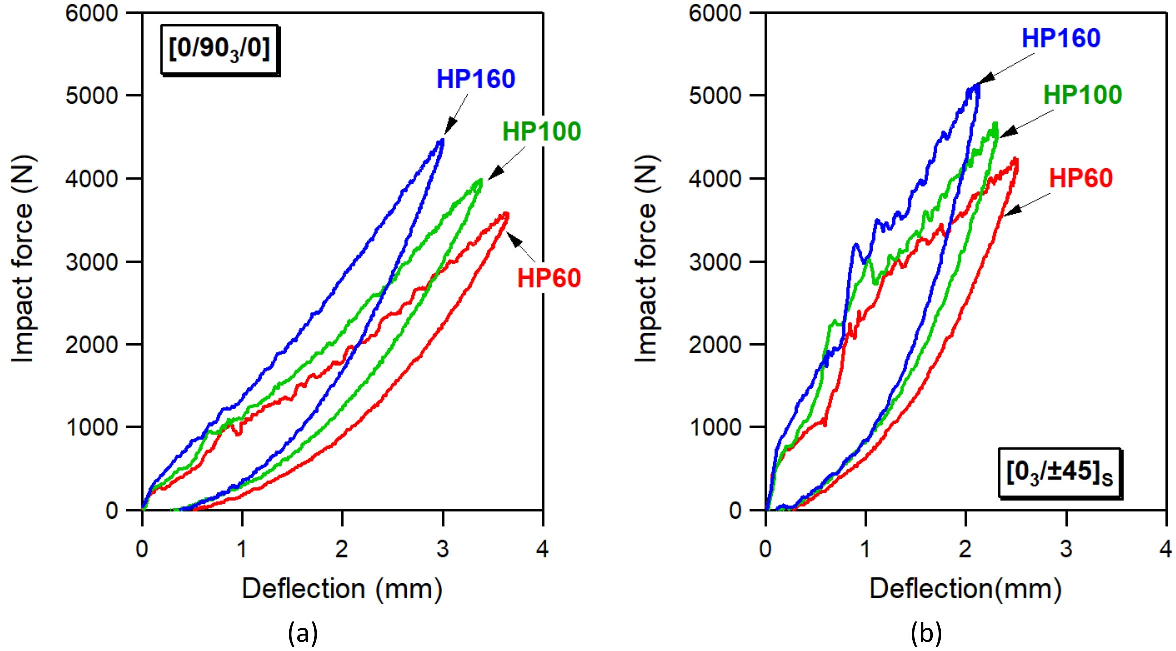

Figure 3: Force-deflection curves of [0/90$_3$/0] (a) and [0$_3$/±45]$_S$ (b) sandwich panels with different core densities for a 6.2 J impact

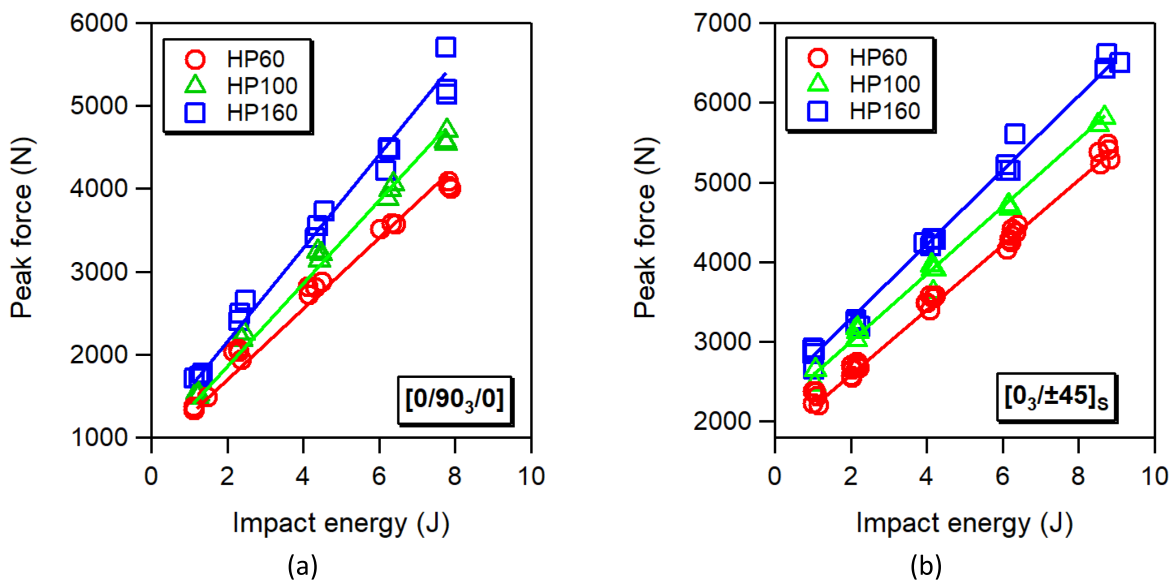

Figure 4: Peak forces measured during impact on [0/90$_3$/0] (a) and [0$_3$/±45]$_S$ (b) sandwich panels with different core densities.

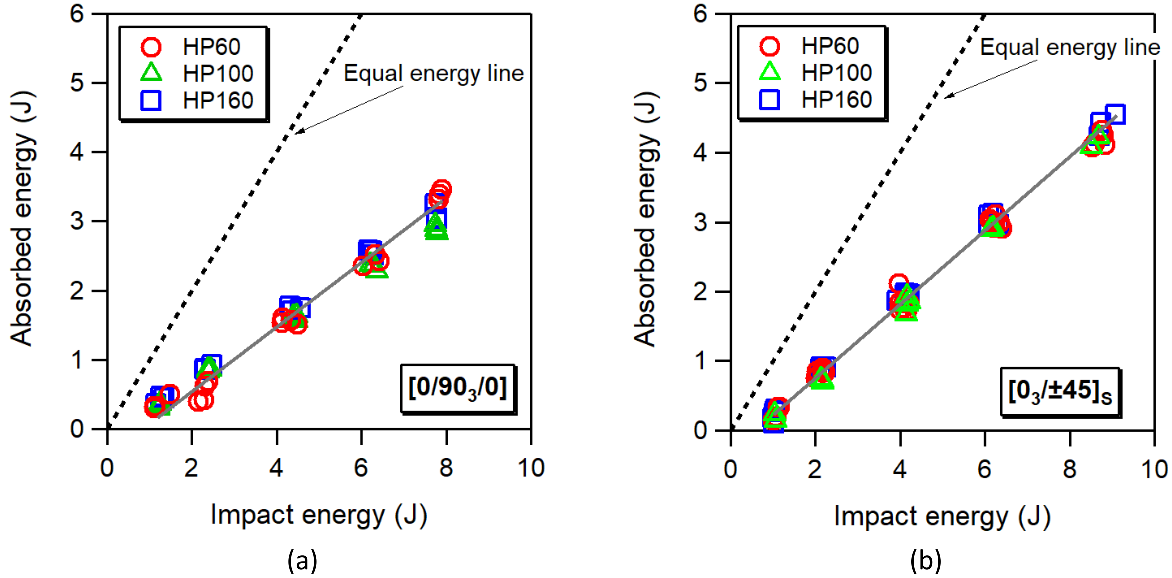

Figure 5: Energies absorbed during impact on $[0/90_3/0]$ (a) and $[0_3/\pm45]_S$ (b) sandwich panels with different core densities. The equal energy line represents the equality between impact energy and absorbed energy.

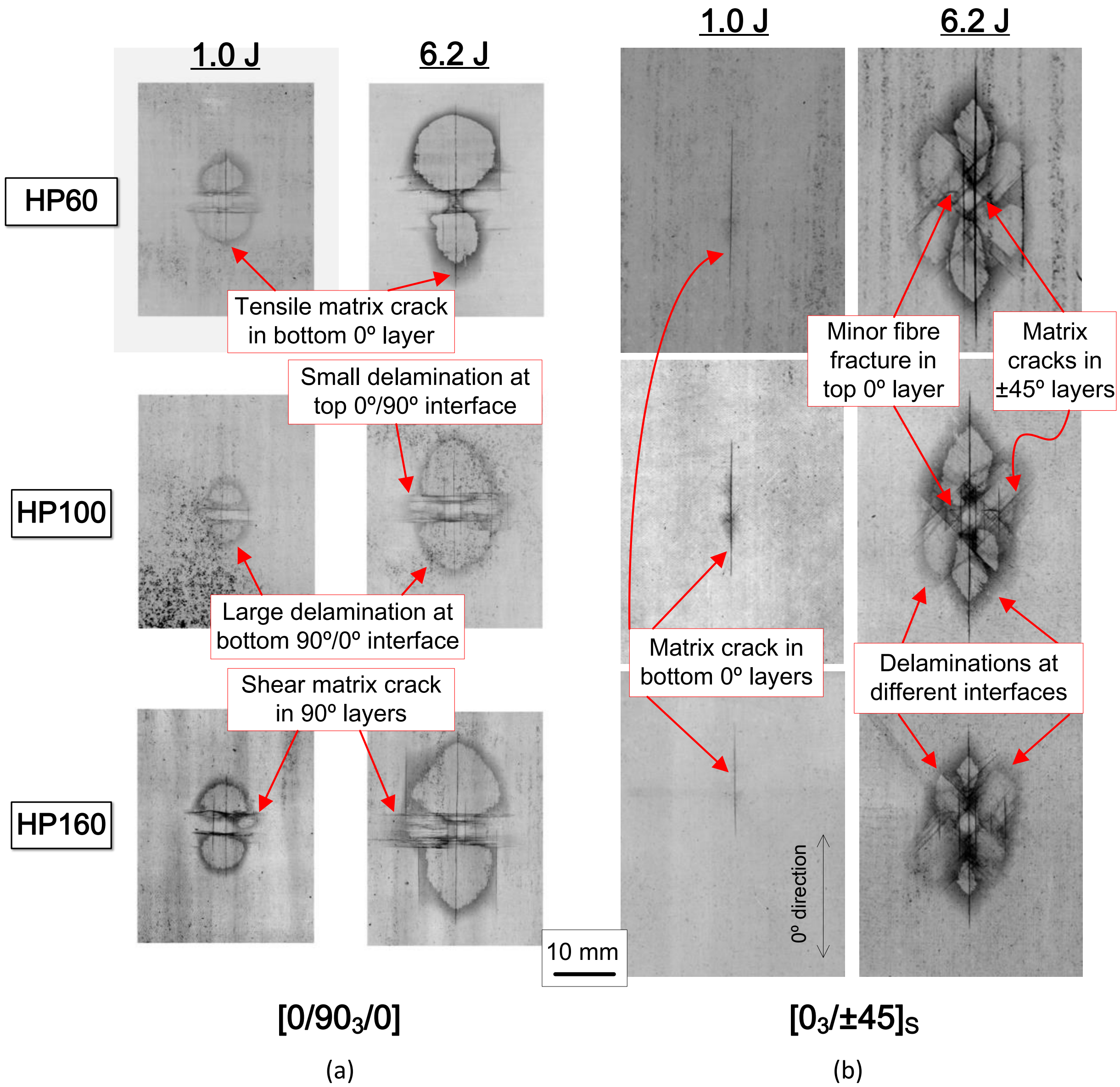

Figure 6: X-radiographs of damage induced by impact on [0/90$_3$/0] (a) and [0$_3$/±45]$_S$ (b) sandwich panels with different core densities.

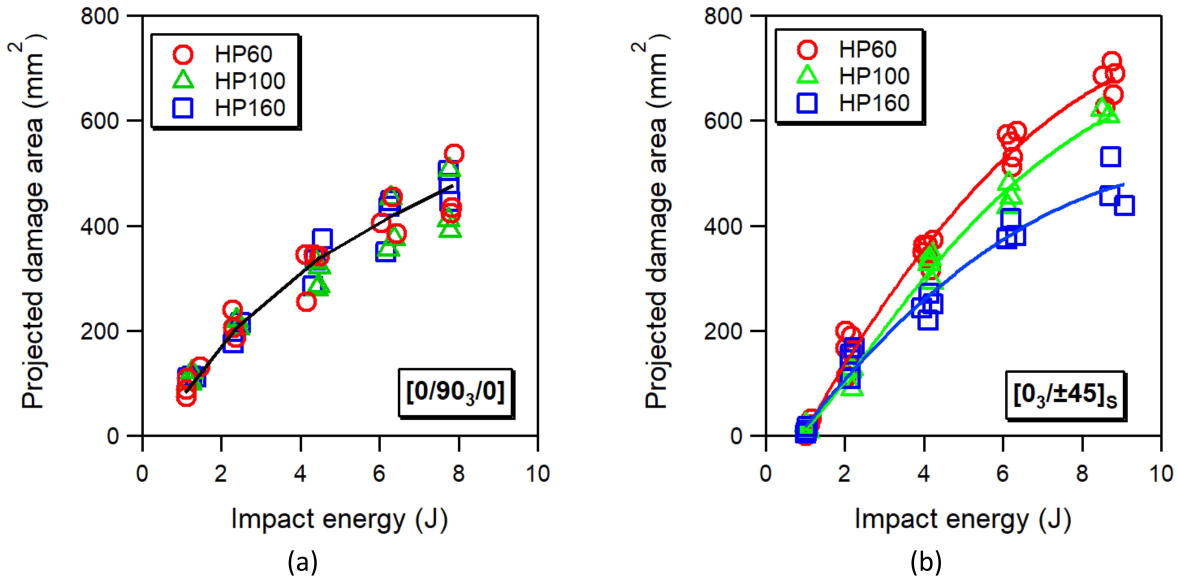

Figure 7: Projected damage areas as a function of impact energy for $[0/90_3/0]$ (a) and $[0_3/\pm45]_S$ (b) sandwich panels with different core densities.

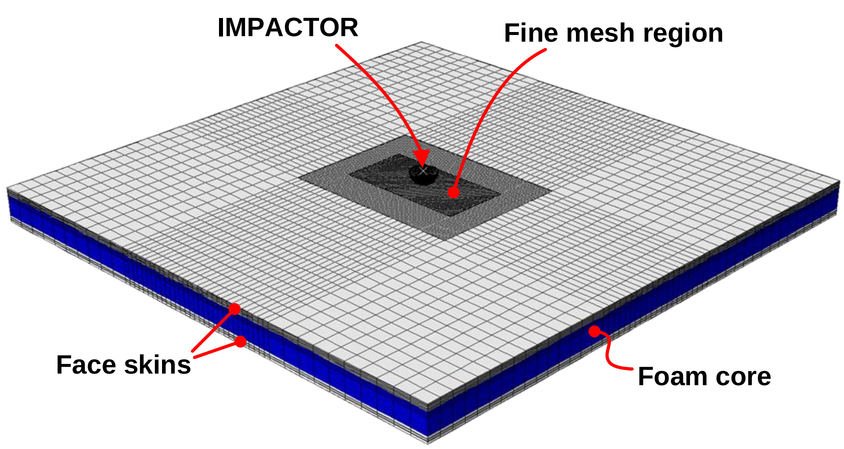

Figure 8: FE model of the composite sandwich panels

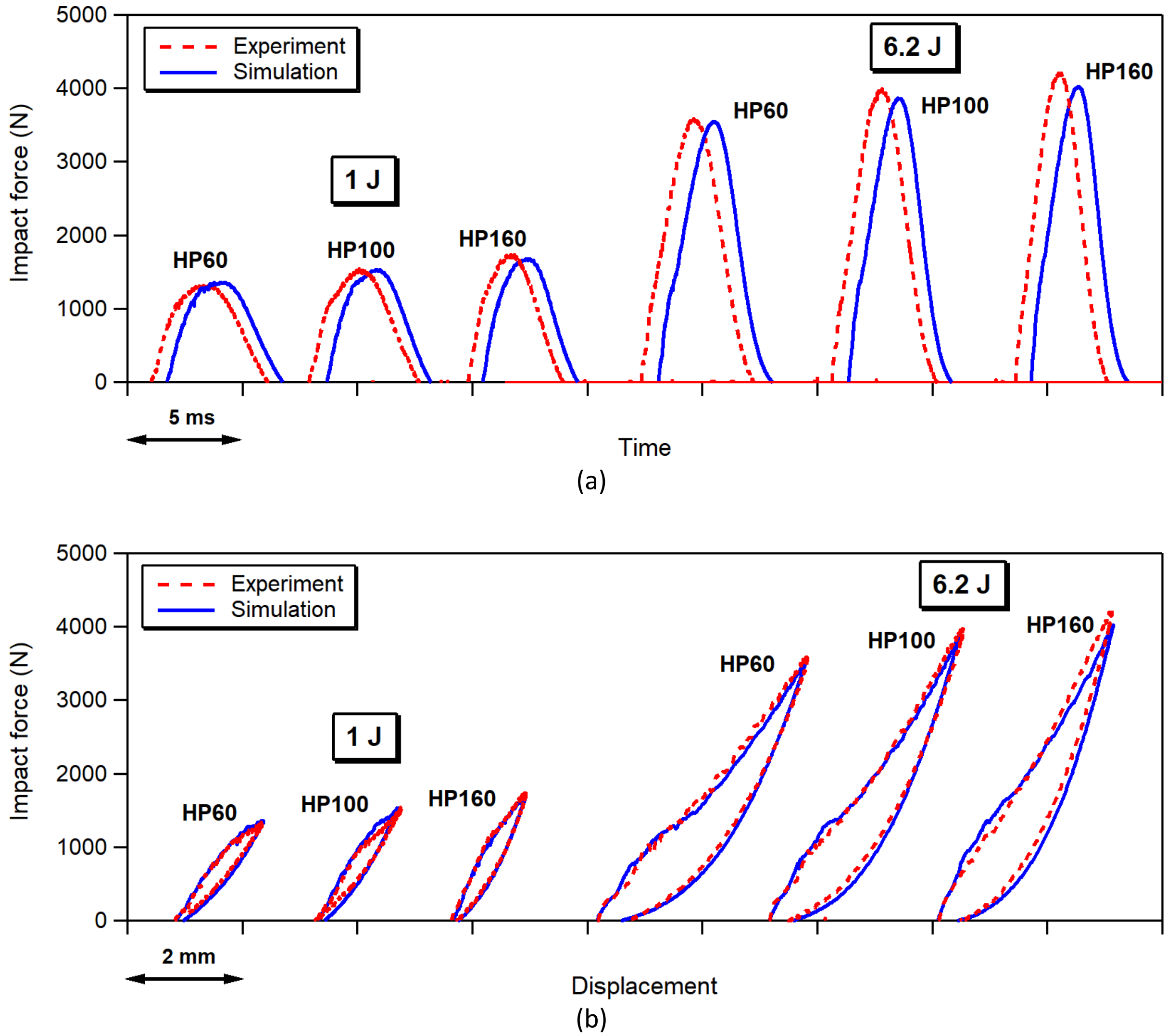

Figure 9: Comparison of experimental and predicted force-time (a) and force-displacement (b) curves for $[0/90_3/0]$ sandwich panels with different core densities.

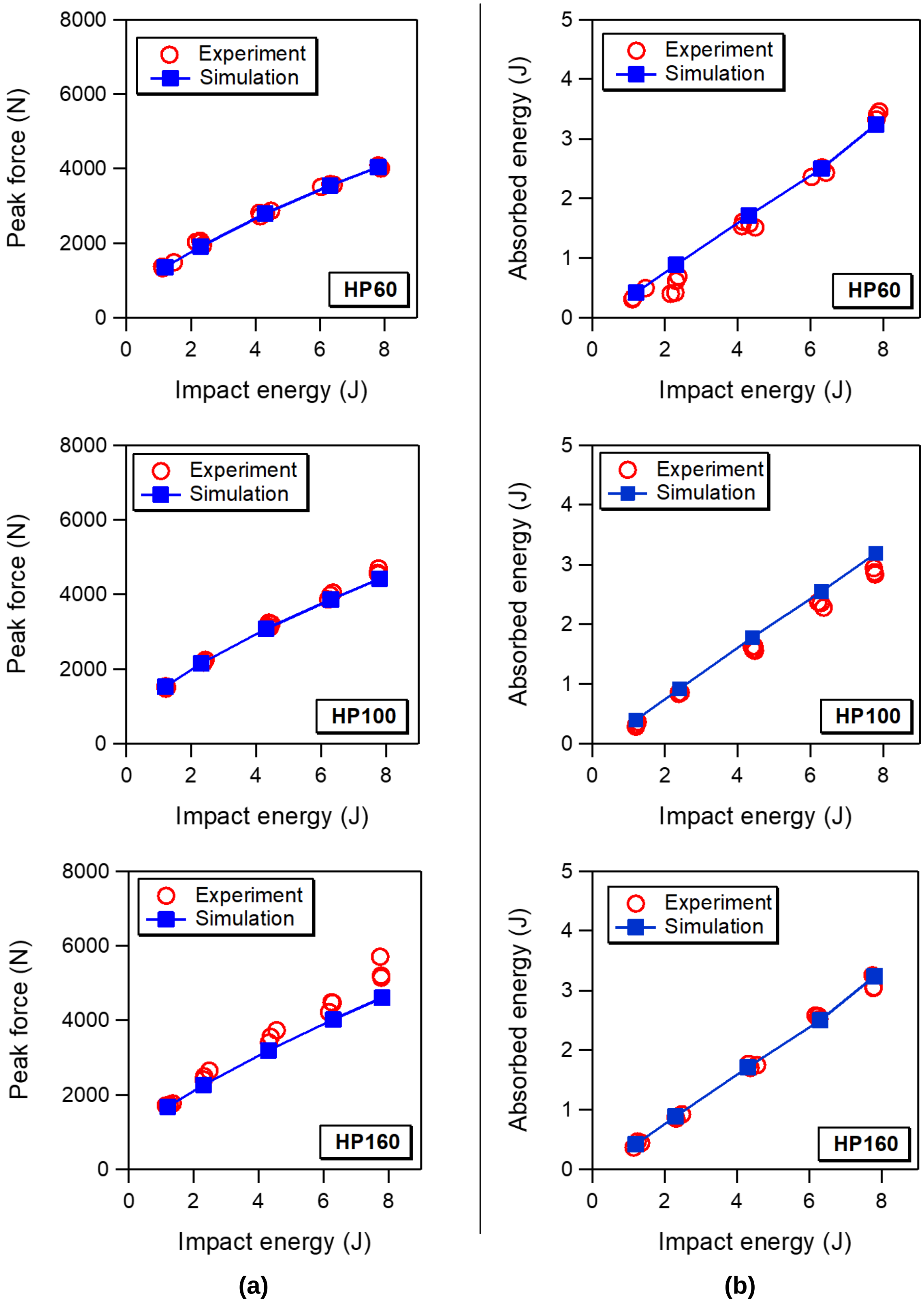

Figure 10: Comparison of experimental and predicted peak force (a) and absorbed energy (b) values for impacts on [0/90$_3$/0] sandwich panels with different core densities.

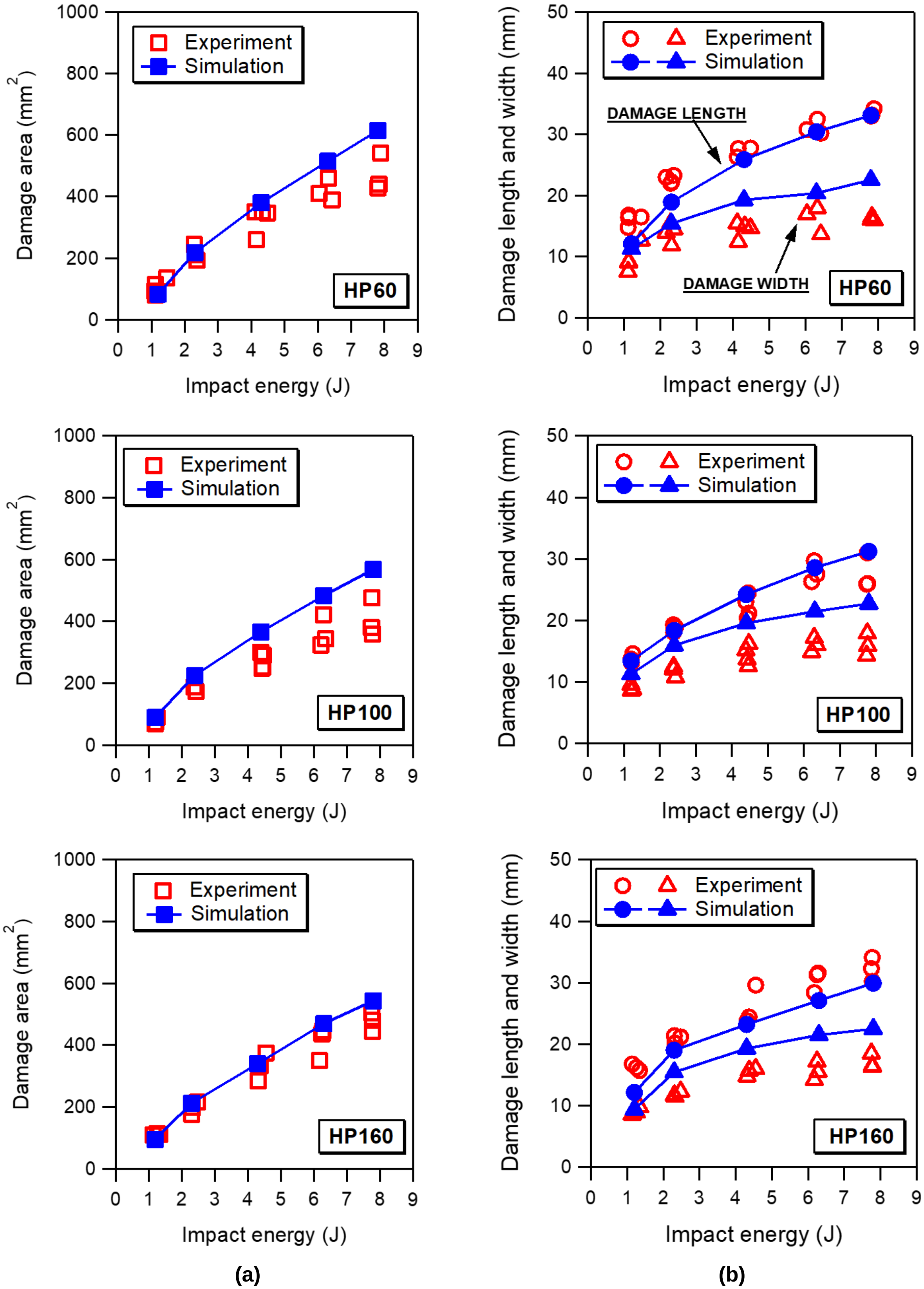

Figure 11: Comparison of experimental and predicted damage area (a) and damage length and width (b) values for impacts on [0/90$_3$/0] sandwich panels with different core densities.

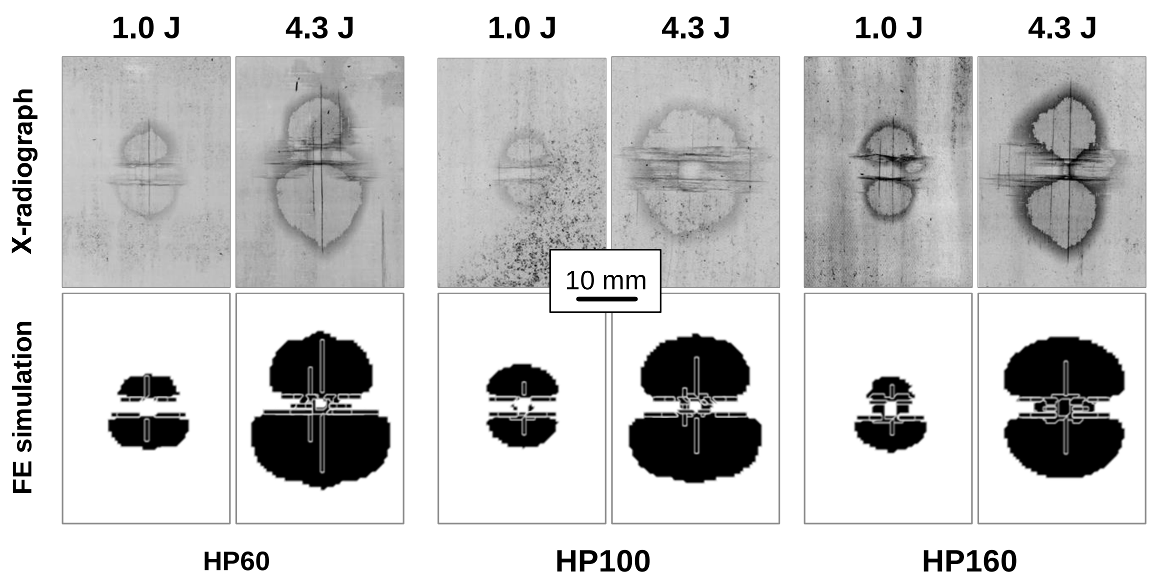

Figure 12: Comparison of experimental and predicted impact damage in $[0/90_3/0]$ sandwich panels with different core densities.

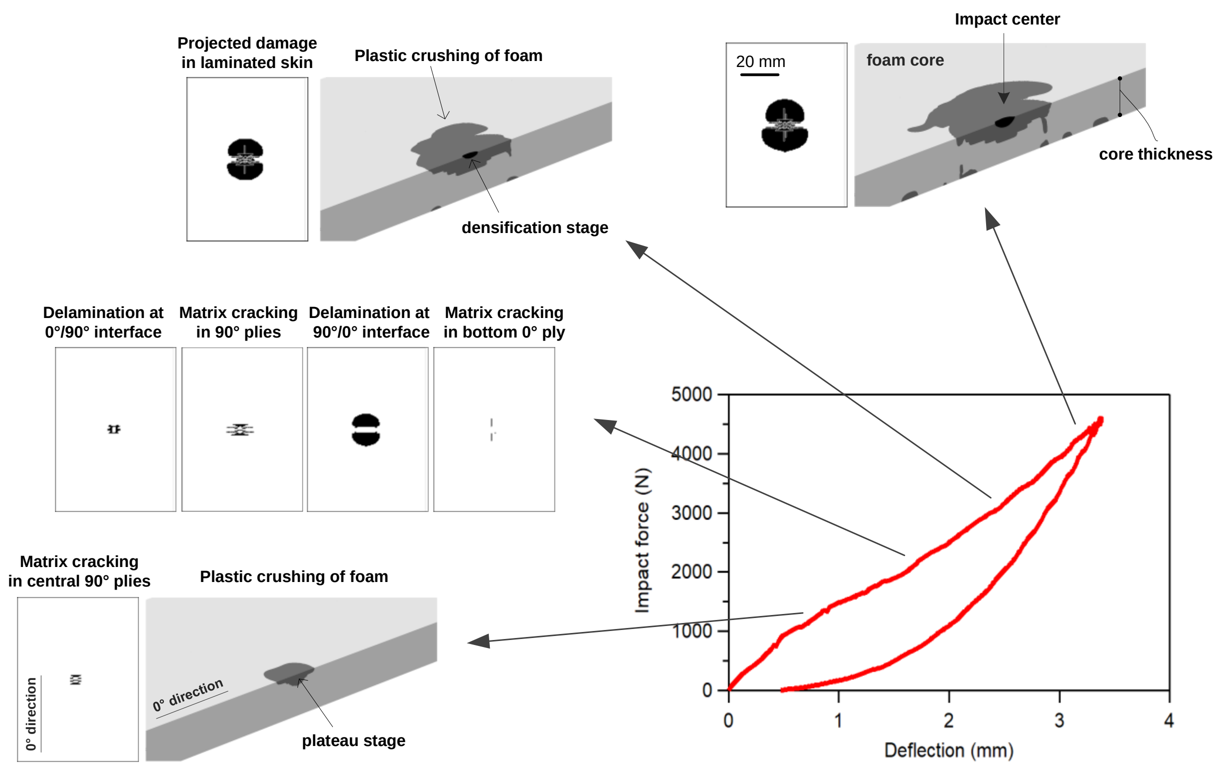

Figure 13: Sequence of damage events predicted by the FE model for a 7.8 J impact on a $[0/90_3/0]$ sandwich panel with HP160 (160 kg/m^3) core.

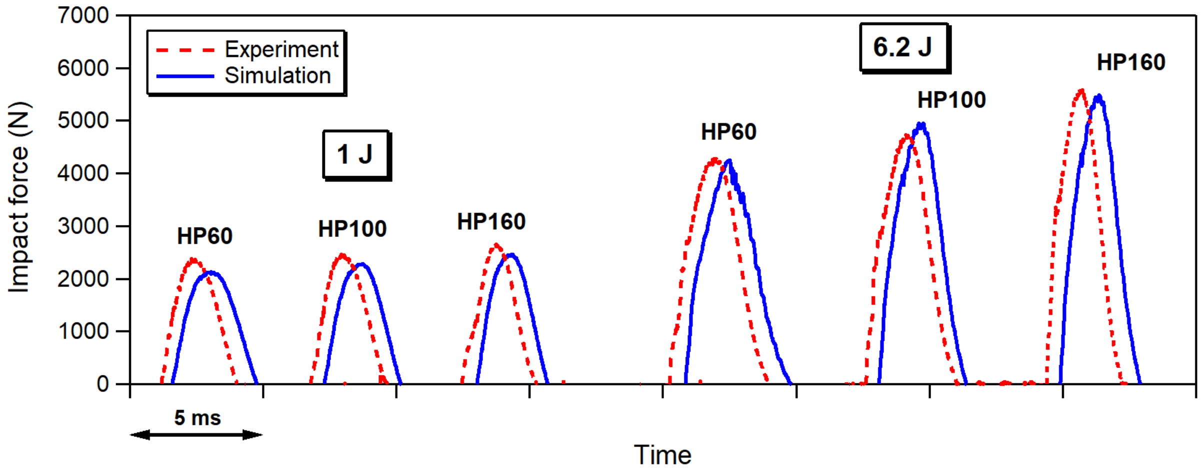

(a)

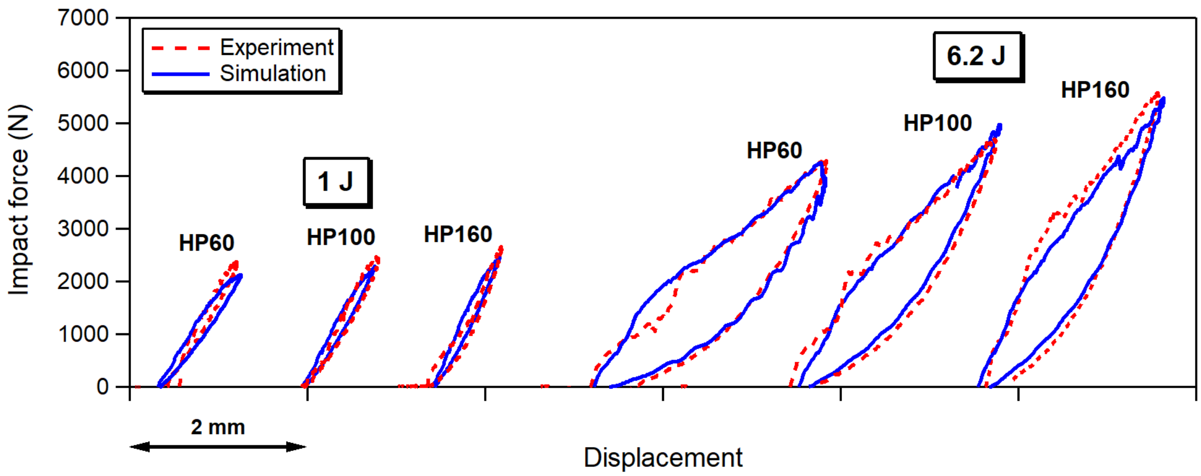

(b)

Figure 14: Comparison of measured and predicted force-time (a) and force-displacement (b) curves for $[0_3/\pm45]_S$ sandwich panels with different core densities.

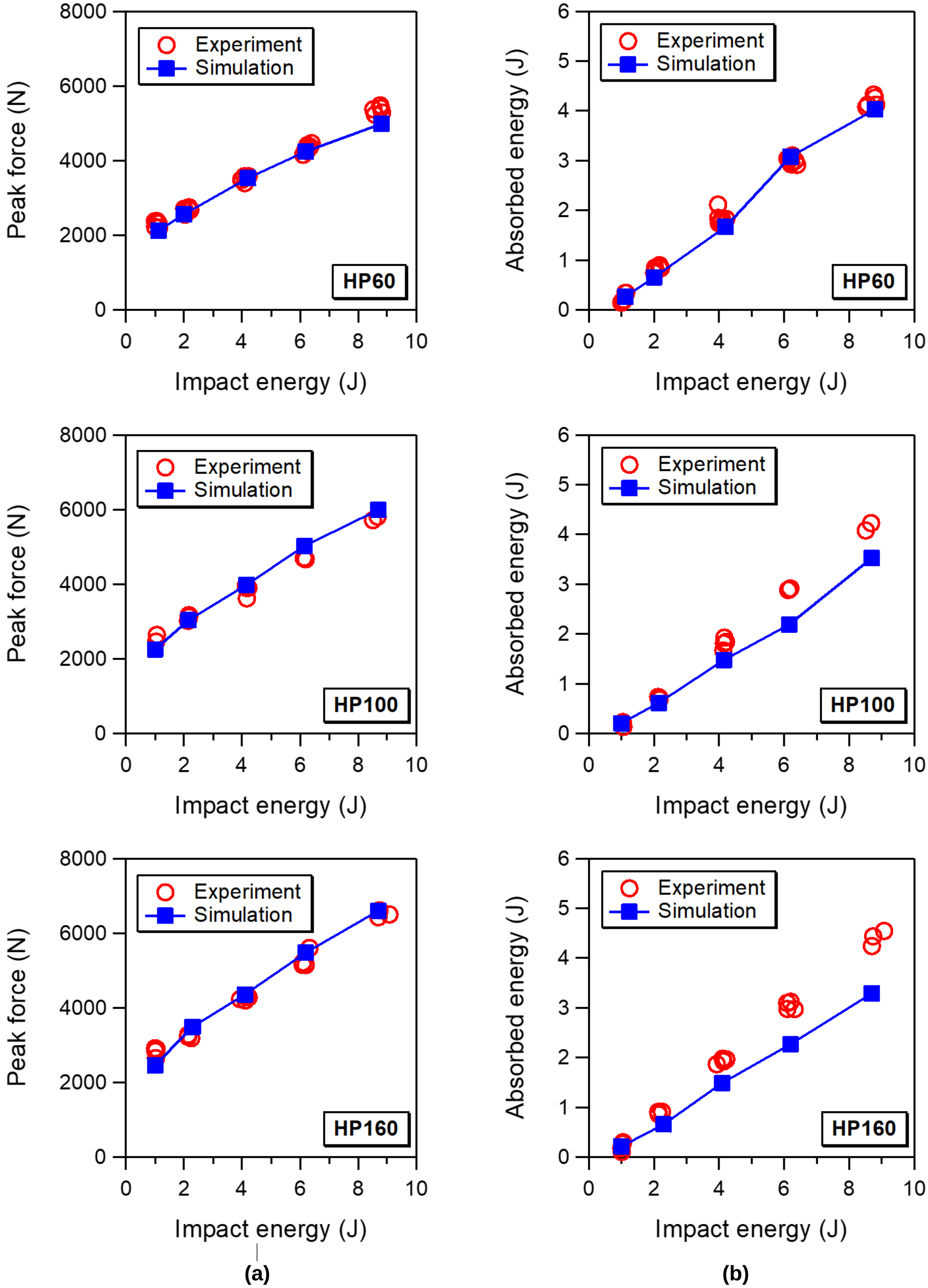

Figure 15: Comparison of experimental and predicted peak force (a) and absorbed energy (b) values for impacts on $[0_3/\pm45]_S$ sandwich panels with different core densities.

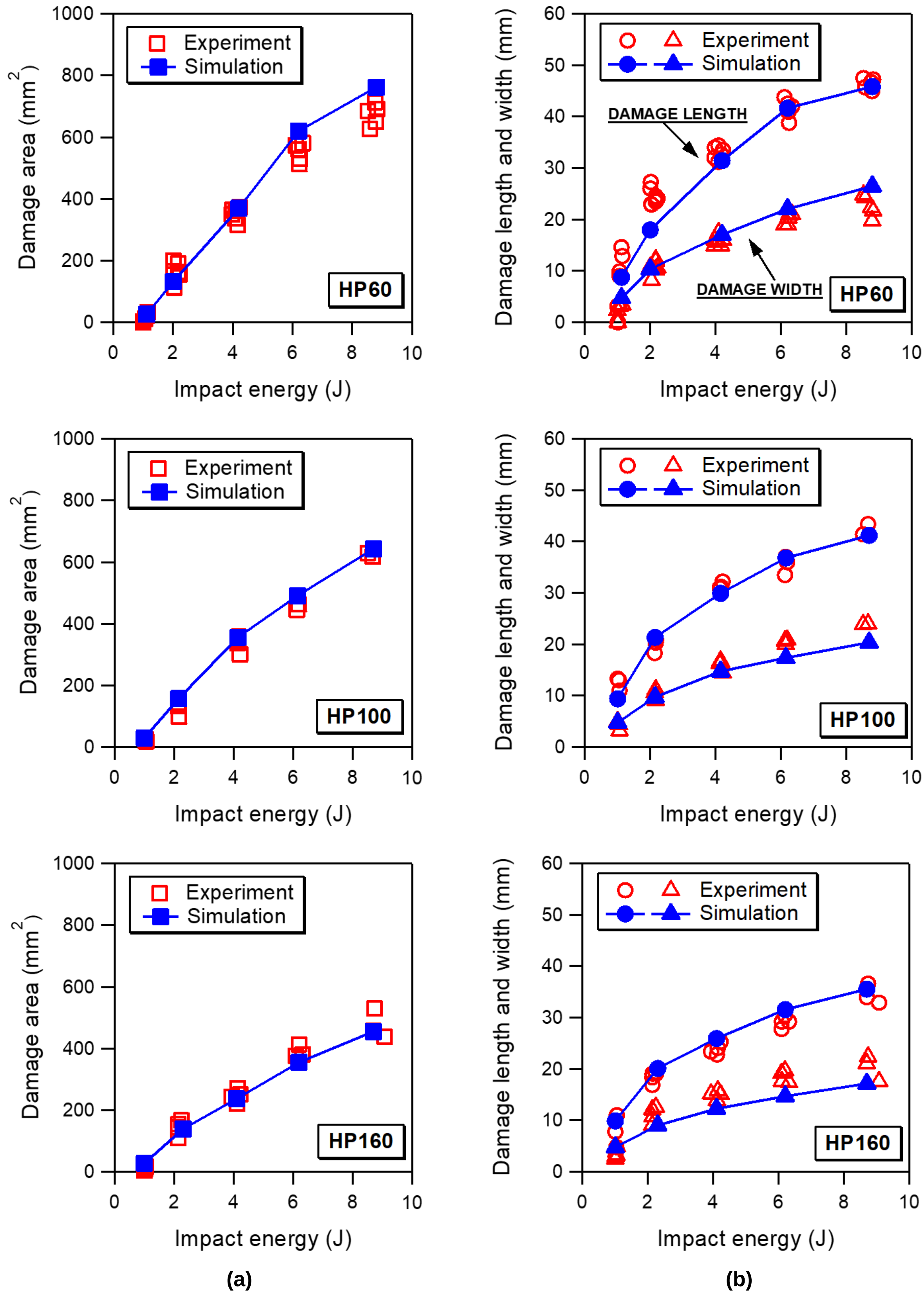

Figure 16: Comparison of experimental and predicted damage area (a) and damage length and width (b) values for impacts on $[0_3/\pm45]_S$ sandwich panels with different core densities.

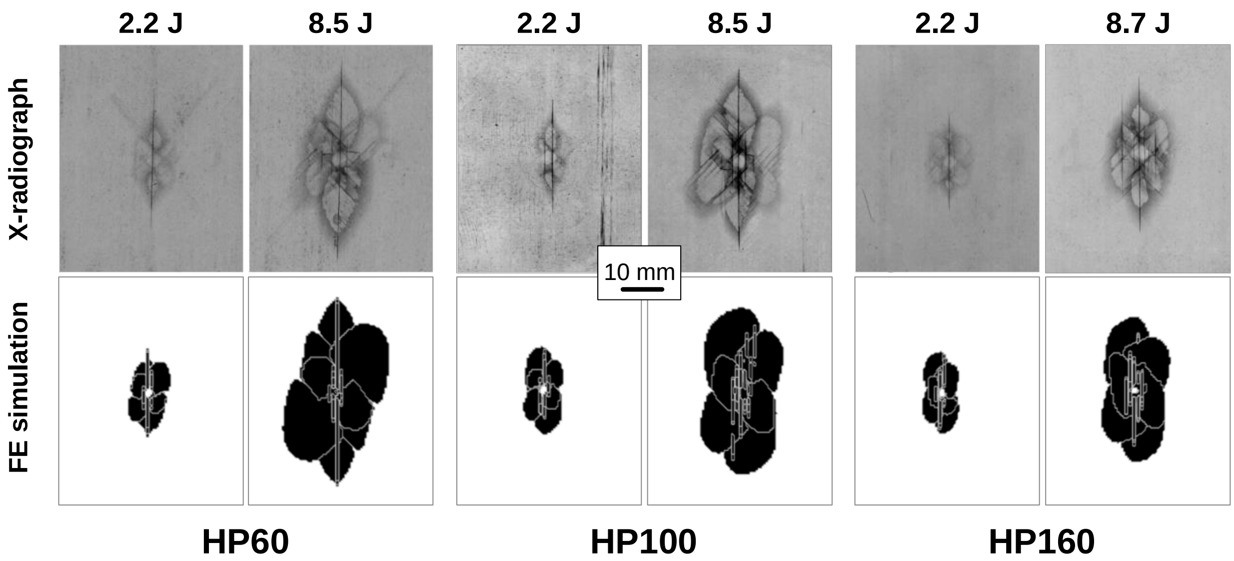

Figure 17: Comparison of experimental and predicted impact damage in $[0_3/\pm45]_S$ sandwich panels with different core densities.

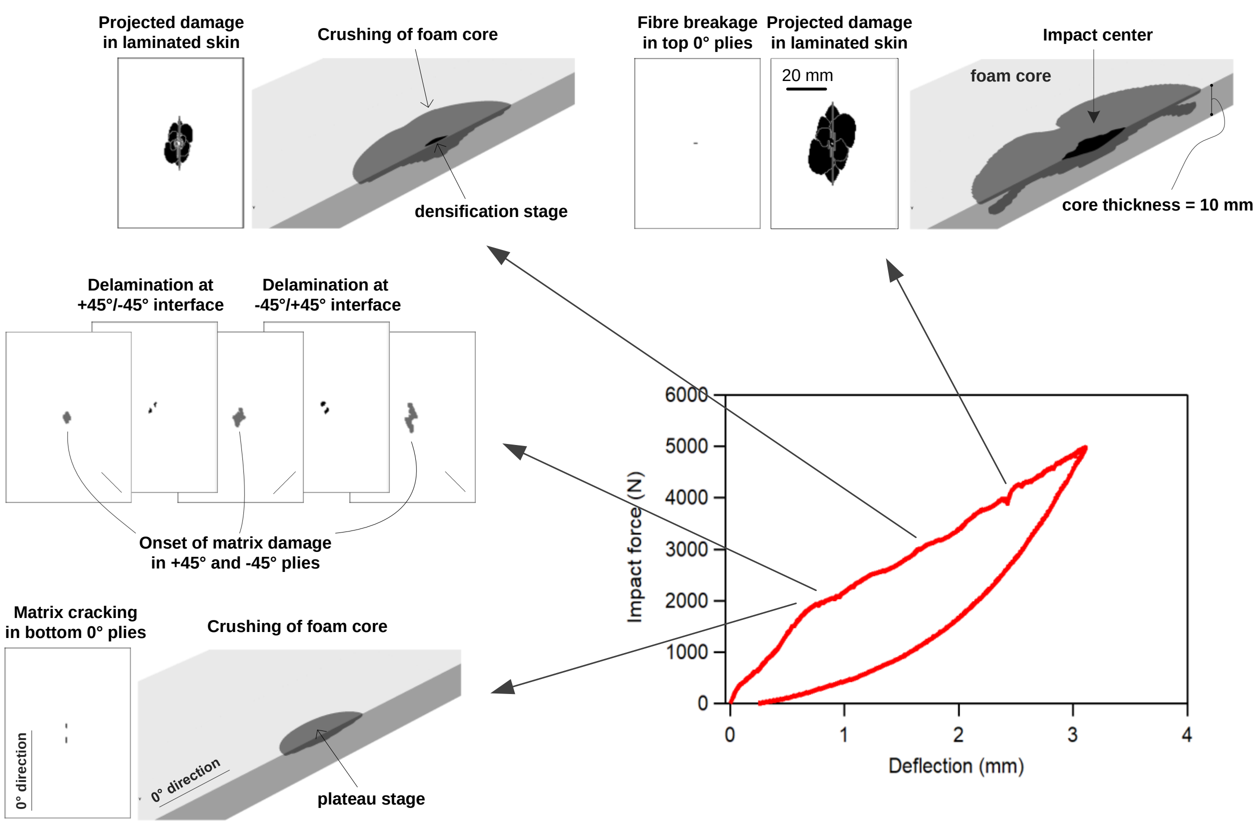

Figure 18: Sequence of damage events predicted by the FE model for a 8.5 J impact on a $[0_3/\pm45]_S$ sandwich panel with HP60 (65 kg/m^3) core.